

Electronic band gaps of diamond nanowires

A. S. Barnard, S. P. Russo,* and I. K. Snook

Department of Applied Physics, Royal Melbourne Institute of Technology University, GPO Box 2476V, Melbourne 3001, Australia

(Received 6 August 2003; published 11 December 2003)

Recent advances in the fabrication and characterization of semiconductor and metallic nanowires are proving very successful in meeting the high expectations of nanotechnologists. Although diamond has been found to possess remarkable electronic and chemical properties, development of diamond nanowires has been slow. Successes in this are expected to increase, making a description of the electronic properties of diamond nanowires of significant importance. In an attempt to predict the electronic properties of diamond nanowires, we have used *ab initio* techniques to calculate the electronic density of states of stable diamond nanowires, with cubic and dodecahedral surface facets. Our results indicate that the energy band gap of diamond nanowires is significantly reduced, due to the contributions from occupied and unoccupied surface states. This reduction is shown to be dependent on the nanowire diameter, surface morphology, and surface hydrogenation.

DOI: 10.1103/PhysRevB.68.235407

PACS number(s): 78.67.Lt, 31.15.Ar, 61.46.+w, 73.22.-f

The emergence of molecular nanotechnology has introduced a wide range of potential applications of nanostructured materials, for a variety of purposes. One-dimensional (1D) nanowires have been proposed as important components, playing an integral part in the design and construction of both electronic and optoelectronic nanodevices.¹ In particular, the electronic properties of nanowires, the *I-V* characteristics, and the degree to which these properties may be manipulated by modifying the nanowire structure are of great interest. Significant work has been compiled regarding the electronic properties of semiconductor nanowires including silicon,^{2,3} silicon carbide,^{4,5} and carbon.⁶⁻¹⁰ Recent advances in the synthesis, characterization, and structural modification of silicon nanowires have shown great promise.

Diamond has been suggested to be the optimal choice for nanomechanical designs, due to its high elastic modulus and strength-to-weight ratio, and relative ease with which surfaces may be functionalized.¹¹ Theoretical comparisons with carbon nanotubes have shown that diamond nanowires are energetically and mechanically viable structures, even at diameters under 5 nm.¹² Aligned diamond nanowhiskers have been successfully formed using air plasma etching of polycrystalline diamond films.¹³ Dry etching of the diamond films with molybdenum deposits created well-aligned uniformly dispersed nanowhiskers up to 60 nm in diameter with a density of 50 μm^{-2} . These diamond nanowhiskers showed well-defined characteristics of diamond.¹³ Diamond nanocylinders with a diameter of ≈ 300 nm have been synthesized,¹⁴ and most recently, “nanorods” of single crystalline diamond have been reported.¹⁵ These predictions and fabrication success stories make the description of the electronic properties of diamond nanowires of significant importance.

As nanowires have very high surface-to-volume ratios the surface structure is central to the electronic properties of these nanostructures. The surface structure of stable cubic diamond nanowires has been examined previously, and has been found to vary significantly over individual surface facets.¹⁶ These surface variations (and more complicated surface disorder) will effect the electronic properties of diamond nanowires, making the band structure differ from that of bulk diamond, especially in the vicinity of the band gap. For this

reason, it is first necessary (in order to gain an understanding of the effects of surface structure upon the band gap) to examine the electronic structure of more homogeneous diamond nanowire surfaces, and to compare to bulk diamond. Only after such a study may the electronic structure of more complicated diamond nanowires be investigated.

A number of papers have been published regarding the electronic structure of both hydrogenated and dehydrogenated bulk diamond C(110) (Ref. 17) and C(100) (Ref. 18) surfaces. Kern and Hafner¹⁷ found using density-functional theory (DFT) within the local-density approximation (LDA) that the C(110) surface produces a number of bonding and antibonding states. The occupied bonding states for the dehydrogenated C(110) surface fall from ≈ 1.0 eV below to 1.0 eV above the valence-band maximum, and were characterized as *pp* π^* states. The *p_z* antibonding states (formed by the dangling surface bonds) were found to form two states situated in the band gap (along the $\overline{\Gamma X}$ direction). These states had a large dispersion of 3.4 eV above the valence-band maximum, thereby reducing the band gap. In the case of the hydrogenated C(110):H surface, these antibonding states were removed, and the C-H states were introduced from 2 eV above the valence-band maximum to merge with the conduction band, also reducing the band gap. Their study concluded that the C(110) surface is metallic whereas the C(110):H surface is semiconducting.

Furthmüller *et al.*¹⁸ conducted a similar (DFT LDA) study on the C(100) and C(100):H surfaces. The dehydrogenated surface was found to produce unoccupied π states in the band gap from ≈ 1.5 eV to 2.5 eV above the valence band maximum Table I. The occupied states fell between -2 eV and 0 eV, below the valence-band maximum. Yang *et al.*¹⁹ (using DF-TB) also found states in the band gap, from 0.5 eV to 3.0 eV from the valence-band maximum. Like the C(110):H surface, hydrogenation was found to remove these states.^{18,19} The C(100):H surface also showed band-gap narrowing, with the C-H bonding states evident from 3.3 eV to 6 eV below the conduction-band minimum, merging with the conduction band.

In the first part of the present study, the electronic properties of diamond nanowires have been investigated as a

TABLE I. Electronic states produced by dehydrogenated and hydrogenated C(100) and C(110) bulk-diamond surfaces, indicating the occupied (bonding) and unoccupied (antibonding) states. All energy ranges are given in reference to the valence-band maximum.

Surface	Occupation	Energy range (eV)
C(100)(2×1)	Occupied	−2.0–0.0
C(100)(2×1)	Unoccupied	1.5–2.7
C(100)(2×1):H	Occupied	3.3–6.0
C(110)(1×1)	Occupied	−1.0–1.0
C(110)(1×1)	Unoccupied	1.0–3.4
C(110)(1×1):H	Occupied	2.0–7.0

function of nanowire diameter and morphology. Three morphologies have been considered consisting of pure dodecahedral and combination cubododecahedral forms, one of which is denoted as “cubic” due to the square or rectangular cross section and the other as “cylindrical” due to the circular cross section. The three dodecahedral nanowires range in average lateral diameter from ~ 0.46 nm to ~ 0.78 nm, consisting entirely of C(110) surfaces with the principle axis in the [100] direction. The three cubic diamond nanowires (with average diameters from ~ 0.45 nm to ~ 0.87 nm) consist of two C(110) surfaces and two C(100) surfaces, and have the principle axis in the [110] direction. Like the cubic nanowires, the five cylindrical diamond nanowires (with average diameters from ~ 0.44 nm to ~ 1.79 nm) consist of four C(110) surfaces and four C(100) surfaces, but with the principle axis in the [100] direction. Each of the nanowires has been structurally relaxed prior to the calculation of properties and determined to be stable in the diamond structure, with the exception of the smallest dehydrogenated cubic nanowire,²⁰ which has therefore been omitted from this study. While these nanowires are ultrafine, and successful synthesis of such nanomaterials may take some time, the use of *ab initio* methods (and currently available computational resources) in this case limits the size of systems that may be studied.

In all, ten dehydrogenated and nine hydrogenated diamond nanowire structures were constructed with periodic boundary conditions applied along the principle axis, and sufficient vacuum space added in the lateral directions to create infinite 1D structures. This gives a sample of structures with two distinct orientations, a variety of surface structures, and a range of sizes. The electronic properties were calculated with the Vienna *ab initio* simulation package,²¹ using DFT within the generalized-gradient approximation (GGA), with the exchange-correlation functional of Perdew and Wang.²² We used ultrasoft, gradient corrected Vanderbilt-type pseudopotentials²³ and expanded the valence orbitals on a plane-wave basis up to a kinetic-energy cutoff of 290.00 eV. This method has been successfully applied to bulk diamond,²⁴ diamond nanowires,¹⁶ nanodiamond,²⁵ and fullerenes,²⁶ and has been shown to give results in excellent agreement with experiment and all electron methods. Preliminary testing determined that a $16 \times 4 \times 4$ Monkhorst-Pack k -point mesh was sufficient in this case, and that no advantage could be gained by using a larger k mesh or plane-wave cutoff. Application of the linear tetrahedron method for Brillouin-zone integration meant that the use of less k points (even in nonperiodic directions) was not recommended.

Although the DFT GGA method may not be the “ideal” method of choice for calculating band gaps, it has been used here for a number of reasons. First, higher levels of theory that give more accurate band-structure results (such as quantum Monte Carlo²⁷) are currently computationally too expensive to make the investigation of the larger diameter nanowires viable. Second, it was considered desirable to obtain results for all of the nanowires considered using the same theoretical technique, to promote consistency and enable cross comparison of the nanowire results. Finally, the application of DFT facilitated direct comparison with the band gaps of bulk-diamond and bulk diamond surfaces obtained by other research groups.^{17,18}

As expected (from knowledge of bulk-diamond surfaces) the electronic density of states (EDOS) of the dehydrogenated dodecahedral nanowires showed additional peaks in

TABLE II. Electronic band gap (E_g) of the dehydrogenated and hydrogenated diamond nanowires, with corresponding diameter (D) and percentage C(110) surface bonds. Hydrogen terminations included in diameters.

Morphology	C(110) (%)	Dehydrogenated		Hydrogenated	
		D (nm)	E_g (eV)	D (nm)	E_g (eV)
Dodecahedral	100	0.46	1.35	0.52	3.08
Dodecahedral	100	0.58	0.54	0.65	2.65
Dodecahedral	100	0.72	0.77	0.78	2.40
Cubic	55.6			0.47	3.50
Cubic	66.7	0.58	1.10	0.61	2.72
Cubic	50.0	0.81	0.89	0.86	2.75
Cylindrical	33.3	0.44	4.08	0.49	4.15
Cylindrical	50.0	0.59	1.29	0.63	3.44
Cylindrical	20.0	0.85	3.27	0.89	3.07
Cylindrical	55.6	1.55	1.80		
Cylindrical	60.0	1.79	3.59		

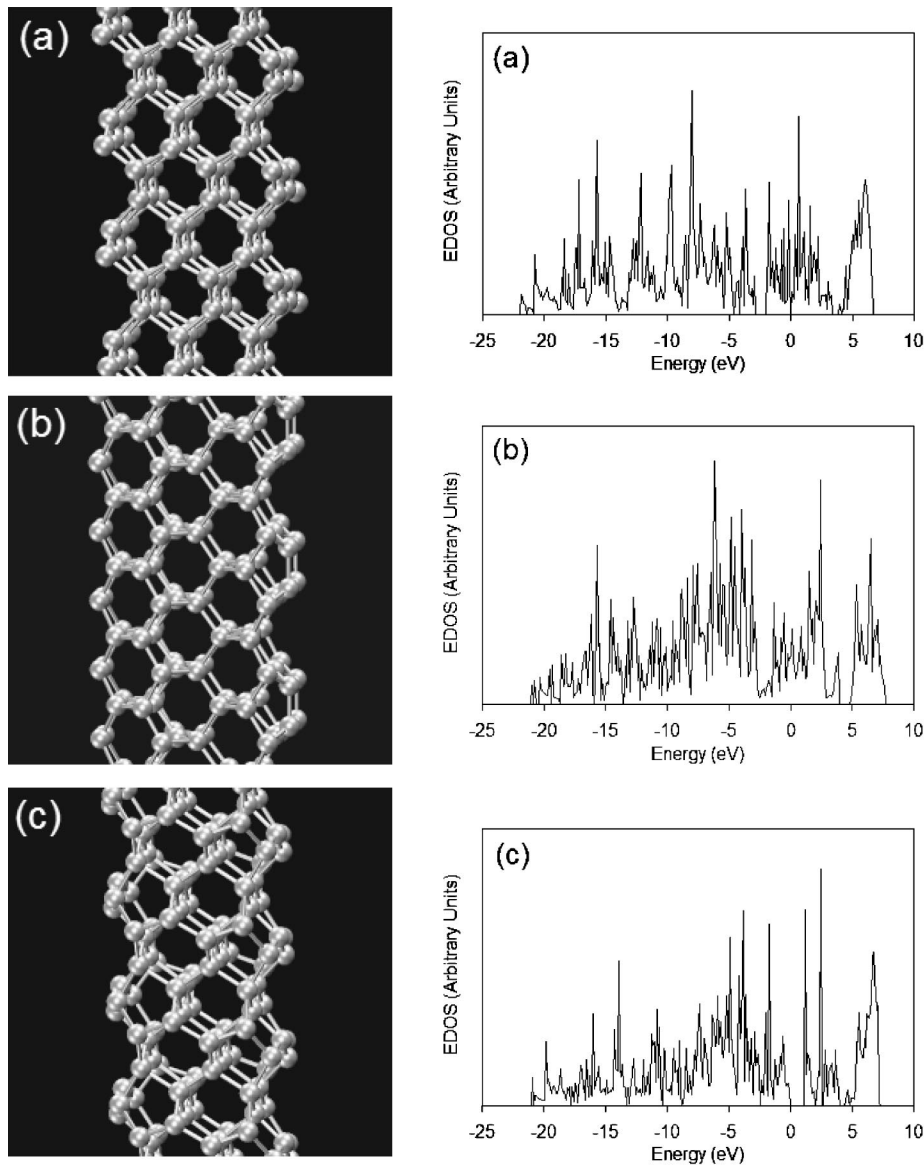


FIG. 1. The structure (left) and EDOS (right) for the dehydrogenated ~ 0.58 nm dodecahedral (a), ~ 0.58 nm cubic (b), and ~ 0.59 nm cylindrical (c) diamond nanowires.

the band gap, due to the addition of unoccupied $C(110)(1 \times 1)$ surface states. These states appear to merge the valence-band maximum, thereby narrowing the band gap. The number of these states increased in the larger dodecahedral nanowires, with the ~ 0.58 -nm dehydrogenated $\{110\}$ structure effectively having the smallest calculated band gap. As an example, the structure and the EDOS for the ~ 0.58 -nm dodecahedral nanowire are given in Fig. 1(a). The small gap at ≈ -2 eV is within the occupied valence band, with occupied states above this range.

The dehydrogenated cubic and cylindrical nanowires also exhibited significant band-gap narrowing due to the introduction of unoccupied $C(100)(2 \times 1)$ and $C(110)(1 \times 1)$ states above the valence-band maximum. The structures and EDOS for the ~ 0.58 -nm cubic nanowire and the ~ 0.59 -nm cylindrical nanowire are shown in Figs. 1(b) and 1(c), respectively. For both the ~ 0.58 -nm and ~ 0.81 -nm cubic structures, significant band narrowing is observed, with the unoccupied $C(100)(2 \times 1)$ and $C(110)(1 \times 1)$ states merging with the valence-band maximum. The band gap of the

~ 0.58 -nm cubic nanowire shown in Fig. 1(b), is zero (and the density of states at the Fermi level is finite) indicating a metal or semimetal. However, in the case the cylindrical nanowires the unoccupied $C(100)(2 \times 1)$ and $C(110)(1 \times 1)$ states are higher than the valence-band maximum. The states in the band gap of ~ 0.59 -nm cylindrical nanowire (although unoccupied) are closer to the conduction band minimum, rather than the valence-band maximum as was observed in the cubic nanowire of the same size, indicating a semiconductor.

In all of the nanowires (irrespective of morphology), the hydrogenated diamond nanowires exhibit a reasonable amount of band-gap narrowing due to the occupied $C(110) \times (1 \times 1):H$ and $C(100)(2 \times 1):H$ states, which merge with the conduction-band minimum. This narrowing is more pronounced in the larger nanowires than the smaller ones, even though the surface-to-volume ratio is lower. Three examples are given in Fig. 2, showing the structure and EDOS for the ~ 0.65 -nm dodecahedral nanowire [Fig. 2(a)], the ~ 0.61 -nm cubic nanowire [Fig. 2(b)], and the 0.63 -nm cylindrical

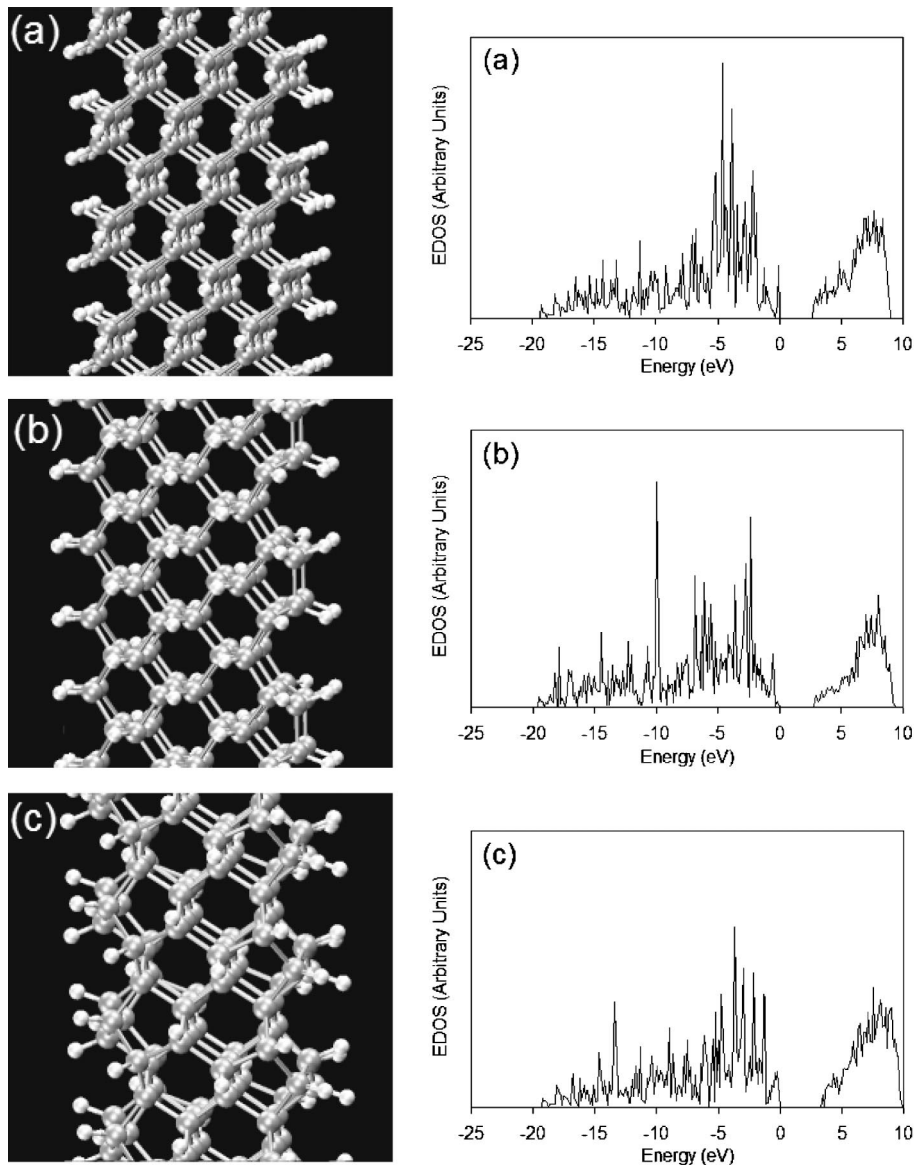


FIG. 2. The structure (left) and EDOS (right) for the hydrogenated ~ 0.65 nm dodecahedral (a), ~ 0.61 nm cubic (b), and ~ 0.63 nm cylindrical (c) diamond nanowires.

nanowire [Fig. 2(c)]. These results are summarized along with the dehydrogenated nanowires in Table II.

The most startling result presented here is dramatic decrease of the band gap, especially in the larger dehydrogenated dodecahedral nanowires. Also, the degree to which this decrease occurs is dependent upon the nanowire diameter, a fact that cannot be merely predicted from knowledge of bulk-diamond surfaces. This, along with the other results listed above, indicated that the presence of the C(110) surfaces (at the nanoscale) has a significant impact on the band gap, for both dehydrogenated and hydrogenated structures. Preliminary result indicates that dehydrogenated nanowires with $>50\%$ C(110) surface bonds are semimetals or metals in this size range, whereas dehydrogenated nanowires with $<50\%$ C(110) surface bonds are semiconductors. To assist in determining the extent of these effects, the indirect band gaps for the dehydrogenated and hydrogenated diamond nanowires considered here have been listed in Table I, along with the percentage of C(110) surface bonds (either dangling or C-H).

By comparing like morphologies (both dehydrogenated and hydrogenated versions), the effective band gap was found to decrease with increasing nanowire diameter. Although (due to computational intensity) the band gaps of the hydrogenated diamond nanowires with a diameter greater than 1 nm are not available at this time, since the calculated bulk-diamond band gap is 5.56 eV (experimental value of 5.48 eV), it is anticipated that at some critical diameter this (decreasing) trend of the hydrogenated nanowire band gaps will reverse, and the band gap increases once again to asymptote to the bulk-diamond value.

By comparing like-diameters (across morphologies) the nanowires with a higher percentage of C(110) surface bonds have a lower band gap than those with a higher percentage of C(100) surface bonds. By considering the largest dehydrogenated structures of each morphology, the band gap is highest for the cylindrical nanowires with only 20% C(110). The gap then decreases considerably when the percentage of C(110) is increased to 50% for the cubic nanowire, and decreases still further when the percentage of C(110) is increased to

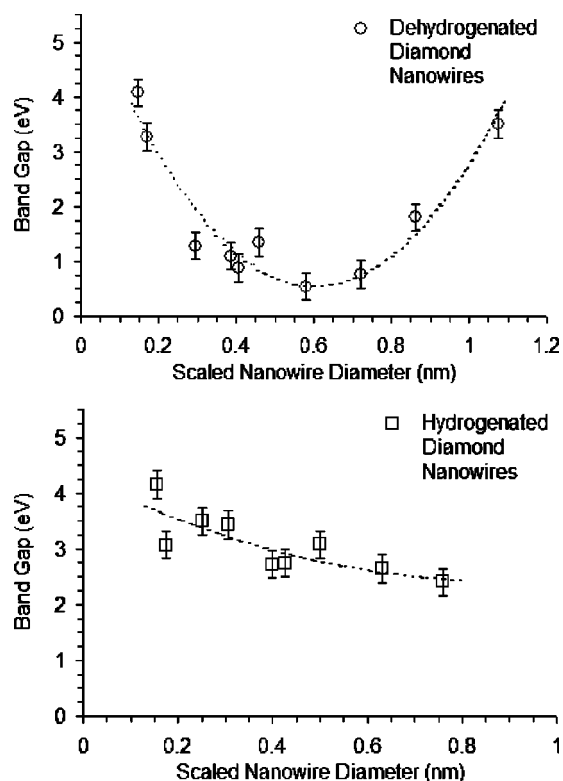


FIG. 3. The electronic band gap vs nanowire diameter scaled by the fraction of C(110) surface bonds for the dehydrogenated (top) and hydrogenated (bottom) diamond nanowires.

100%. A similar trend is evident in the hydrogenated versions.

In an attempt to define some kind of predictable relationship, based on the assumption that the band gap is influenced by the nanowire diameter and the fraction of C(110) surface area [as the C(110) surfaces of bulk diamond are metallic¹⁷], all of the data has been combined. The band gaps for the dehydrogenated and hydrogenated nanowires have been plotted as a function of the average diameter of each nanowire, scaled by the fraction of C(110) surface area. These plots are given in Figs. 3(a) and 3(b) for the dehydrogenated and hydrogenated nanowires, respectively. The dispersion evident in the plots is believed to be due to variations in the surface structure of the nanowires, especially in the vicinity of the edges of the surface facets.¹⁶ The smallest structures effectively have “only edges” as all surface atoms are positioned at a facet edge; however the larger nanowires have more generous surface facets, with relatively fewer atoms positioned at facet edges.

In each case the empirical best fits were found to be quadratic. By solving for the minima it was determined that for

the band-gap minimum, the scaled diameter of dehydrogenated nanowires was ~ 0.61 nm, and of hydrogenated nanowires was ~ 0.90 nm. Assuming that a general nanowire may be synthesized with 50% C(110) surface area, this equates to a dehydrogenated nanowire diameter of ~ 1.22 nm, and a hydrogenated nanowire diameter of ~ 1.81 nm. At these diameters, the predicted band gaps are ~ 0.45 eV, and ~ 2.42 eV, respectively. As the dehydrogenated diamond nanowire band gaps increase beyond this point (and the hydrogenated diamond nanowire band gaps are expected to increase beyond this point), the diameter at which the band gaps equal the calculated bulk-diamond band gap of 5.56 eV [assuming 50% C(110) surface area] occurs at ~ 2.39 nm and ~ 4.14 nm for the dehydrogenated and hydrogenated nanowires, respectively.

Although the reason for the presence of the minimum in the band gap is still under investigation, it is currently thought that the minimum is caused by the presence of the unoccupied surface and edge states in the gap, and the increase above this value (for nanowires with a larger diameter) is due to the decrease in the dispersion induced by the nanowire edges (and their proximity to one another). It is also thought that the increase in the band gap below the minimum value (for nanowires with a smaller diameter) occurs due to quantum confinement effects,²⁸ although this has not yet been confirmed.

In conclusion, it has been determined that the band gaps of diamond nanowires with diameters less than 1.8 nm are significantly smaller than bulk diamond. In dehydrogenated nanowires this reduction in the band-gap is due to the introduction of unoccupied surface states in the gap, whereas for hydrogenated nanowires the band gap narrowing is due to the introduction of occupied surface states near the conduction-band minimum. Our results indicate that the band gap of diamond nanowires may be semiconducting to semimetallic or metallic, depending upon the nanowire diameter, surface morphology, and degree of surface hydrogenation, as well as combinations of these factors. It is therefore suggested that the band gap of diamond nanowires may be engineered to a desired width by skillful manipulation of these structural parameters. Current work is underway to determine the extent to which this is possible, specifically by considering larger nanowire structures, by examining the relationship between the band gap and surface inhomogeneities and applying more sophisticated levels of theory.

We would like to thank the Victorian Partnership for Advanced Computing and the Australian Partnership for Advanced Computing supercomputer center for their ongoing support.

*Electronic address: salvy.russo@rmit.edu.au

¹D. Appell, *Nature (London)* **419**, 553 (2002).

²Y.F. Zhang, L.S. Liao, W.H. Chan, and S.T. Lee, *Phys. Rev. B* **61**, 8298 (2000).

³Z. Zhang, X.H. Fan, L. Xu, C.S. Lee, and S.T. Lee, *Chem. Phys. Lett.* **337**, 18 (2001).

⁴W. Shi, Y. Zheng, H. Peng, N. Wang, C.S. Lee, and S.T. Lee, *J. Am. Ceram. Soc.* **83**, 3228 (2000).

⁵Z. Pan, H.L. Lai, F.C.K. Au, X. Duan, W. Zhou, W. Shi, N. Wang, C.S. Lee, N.B. Wong, S.T. Lee, and S. Xie, *Adv. Mater. (Weinheim, Ger.)* **12**, 1187 (2000).

⁶Y.H. Tang, N. Wang, Y.F. Zhang, C.S. Lee, I. Bello, and S.T. Lee,

- Appl. Phys. Lett. **75**, 2921 (1999).
- ⁷R.Q. Zhang, S.T. Lee, C.-K. Law, W.-K. Li, and B.K. Teo, Chem. Phys. Lett. **364**, 251 (2002).
- ⁸B.O. Boskovic, V. Stolojan, R.U.A. Khan, S. Haq, and R.P. Silva, Nat. Mater. **1**, 165 (2002).
- ⁹S. Botti, R. Ciardi, M.L. Terranova, S. Piccirillo, V. Sessa, and M. Rossi, Chem. Phys. Lett. **355**, 395 (2000).
- ¹⁰A. Xia, Z. Huizhao, Y. Li, and X. Chengshan, Appl. Surf. Sci. **193**, 87 (2002).
- ¹¹O.A. Shenderova, V.V. Zhirnov, and D.W. Brenner, Crit. Rev. Solid State Mater. Sci. **27**, 227 (2002).
- ¹²O.A. Shenderova, D.W. Brenner, and R.S. Ruoff, Nano Lett. **3**, 805 (2003).
- ¹³E.-S. Baik, Y.-J. Baik, S.W. Lee, and D. Jeon, Thin Solid Films **377-378**, 295 (2000).
- ¹⁴H. Masuda, T. Yanagishita, K. Yasui, K. Nishio, I. Yagi, T.N. Rao, and A. Fujishima, Adv. Mater. (Weinheim, Ger.) **13**, 247 (2001).
- ¹⁵Y. Ando, Y. Nishibayashi, K. Kobashi, and A. Sawabe (unpublished).
- ¹⁶A.S. Barnard, S.P. Russo, and I.K. Snook, Surf. Sci. **538**, 204 (2003).
- ¹⁷G. Kern and J. Hafner, Phys. Rev. B **56**, 4203 (1997).
- ¹⁸J. Furthmüller, J. Hafner, and G. Kresse, Phys. Rev. B **53**, 7334 (1996).
- ¹⁹S.H. Yang, D.A. Drabold, and J.B. Adams, Phys. Rev. B **48**, 5261 (1993).
- ²⁰A.S. Barnard, S.P. Russo, and I.K. Snook, Nano Lett. **3**, 10 000 (2003).
- ²¹G. Kresse and J. Hafner, Phys. Rev. B **54**, 11 169 (1996).
- ²²J. Perdew and Y. Wang, Phys. Rev. B **45**, 13 244 (1992).
- ²³D. Vanderbilt, Phys. Rev. B **41**, 7892 (1990).
- ²⁴A.S. Barnard, S.P. Russo, and I.K. Snook, Philos. Mag. B **82**, 1767 (2002).
- ²⁵A.S. Barnard, S.P. Russo, and I.K. Snook, Philos. Mag. Lett. **83**, 39 (2003).
- ²⁶A.S. Barnard, S.P. Russo, and I.K. Snook, J. Chem. Phys. **118**, 5094 (2003).
- ²⁷W.M.C. Foulkes, L. Mitas, R.J. Needs, and G. Rajagopal, Rev. Mod. Phys. **73**, 33 (2001).
- ²⁸Y.K. Chang, H.H. Hsieh, W.F. Pong, M.-H. Tsai, F.Z. Chien, P.K. Tseng, L.C. Chen, T.Y. Wang, K.H. Chen, D.M. Bhusari, J.R. Yang, and S.T. Lin, Phys. Rev. Lett. **82**, 5377 (1999).